

General Anesthetic-induced Seizures Can Be Explained by a Mean-field Model of Cortical Dynamics

Marcus T. Wilson, Ph.D.,* James W. Sleight, M.D.,† D. Alistair Steyn-Ross, Ph.D.,‡ Moira L. Steyn-Ross, Ph.D.§

GENERAL anesthesia is a state in which cerebral activity is usually profoundly suppressed. It is paradoxical that some general anesthetic agents—drugs whose primary action is to decrease central nervous system activity and that have been widely used to treat seizures—can also provoke cortical seizures when the patient is deeply anesthetized.¹⁻³ Traditionally, the explanation for this phenomenon has been sought at a molecular or synaptic level of description, by finding differences between general anesthetic drugs that commonly precipitate seizure activity and those drugs that do not cause seizures. It has been suggested that proconvulsant drugs (such as enflurane) may (1) act to decrease the amplitude of miniature inhibitory postsynaptic currents⁴ or (2) elicit greater calcium-induced presynaptic mobilization of excitatory neurotransmitters⁵ than anticonvulsant drugs (such as isoflurane or thiopentone). These descriptions are qualitative. Are these observations of true causative mechanisms of seizure genesis, or are they simply observations of epiphenomena? It is not clear exactly how these observations at synaptic and molecular scales would quantitatively result in repetitive synchronous widespread burst firing of cortical neurons—the signature of seizure activity.⁶ In this article, we describe a mathematical model of cerebral cortical function (the so-called mean-field model). In our model, we are able to input the known molecular-scale effects of anesthetic drugs and see how they alter the output (a “pseudoencephalogram”) of the computer-simulated “pseudocortex.” We incorporate the values of inhibitory postsynaptic potential (IPSP) amplitude and duration that have been previously published and studied in detail for isoflurane and enflurane, and we compare the output from simulations

run on our theoretical mathematical model with various experimental and clinical observations that have been previously reported in the scientific literature. We find that subtle changes in the shape of the IPSP—induced by enflurane—are sufficient to cause the model of the cerebral cortex to undergo a sudden change in behavior from a general anesthetic state (in which neuronal firing is suppressed) into a seizure-like state—manifest as oscillation between neuronal silence and supramaximal neuronal firing. We use the example of enflurane-induced seizures as a dramatic demonstration of the application of mean-field models of cortical dynamics to link molecular and macroscopic descriptions of nervous system phenomena.

Modeling Cortical Activity

Many neurobiologic phenomena arise predominantly from interactions between and within populations of neurons, rather than directly from the properties of individual neurons. It is necessary to develop a theoretical framework in which to make sense of the experimental observations of these phenomena. What is the best model? Clearly there are many answers to this question. At one extreme are “bottom-up” models that concentrate entirely on biologic accuracy. These take the form of intensely detailed multicompartamental simulations of current flux in each channel in each neuron, and the exact neuronal morphology and connections. This may be termed the neuron-by-neuron approach. At the other end of the spectrum is the abstract neural network/computational approach. In these models, the only interest is in the flow of information, and they barely acknowledge any details of the real underlying biologic “hardware.” The mean-field model—a standard method of analysis in statistical physics—is a compromise between these two extremes. It assumes that the important aspects of neuronal function can be described by the average behavior of a small population of perhaps 10⁵ neurons. Its advantages over the neuron-by-neuron methods are as follows:

1. Mean-field models are computationally manageable without a supercomputer cluster. In contrast, neuron-by-neuron methods for the cortex would involve solving approximately 10-100 sets of equations for up to 100 billion neurons, and a 100 trillion synapses in time steps of much less than 1 ms.
2. The simplification inherent in the mean-field model

◆ This article is accompanied by an Editorial View. Please see: Sceniak MP, MacIver MB: Anesthesia *in silico*. ANESTHESIOLOGY 2006; 104:400-2.

* Lecturer, ‡ Senior Lecturer, § Associate Professor, Department of Physics and Electronic Engineering, University of Waikato. † Professor, Department of Anesthesia, Waikato Clinical School, University of Auckland, Waikato Hospital, Hamilton, New Zealand.

Received from the Department of Physics and Electronic Engineering, University of Waikato, Hamilton, New Zealand. Submitted for publication July 6, 2005. Accepted for publication November 17, 2005. Supported by the Royal Society of New Zealand, Marsden Fund, Wellington, New Zealand, and internal departmental funding.

Address correspondence to Dr. Sleight: Department of Anesthesia, Waikato Clinical School, University of Auckland, Waikato Hospital, Pvt Bag, Hamilton, New Zealand. sleighj@waikatodhb.govt.nz. Individual article reprints may be purchased through the Journal Web site, www.anesthesiology.org.

requires the modeler to try to extract the important components of the neuronal function and interactions on the basis of previous knowledge. This abstraction allows multiple redundant systems (which seem to be common in the central nervous system) to be simply modeled. For example, neuronal excitability may be increased by a large number of neuromodulators acting *via* a plethora of mechanisms (*e.g.*, intracellular, ligand-gated, metabotropic receptors, or even *via* the glia). In most cases, the end effect on the activity of the neuron is similar for all of these mechanisms and can be included in the mean-field model simply as a change in the sigmoid curve that describes the soma potential-to-firing rate relation—the average irritability of the neurons.

3. The output variable of the mean-field model is the mean soma potential of a population of neurons. This can be directly related to the easiest experimentally observed measure of cortical function—the electroencephalogram.

Description of the Mean-field Model

In the mean-field approach, the inputs and responses of individual neurons are replaced by population means. The mean-field model of the interactions between inhibitory and excitatory cortical neuronal populations has been previously used to describe the electroencephalographic effects of general anesthesia and sleep and has been described in detail in a recent article by Wilson *et al.*⁷ A synopsis is presented in the appendix to this article. It builds on a previous body of work by Liley, Wright, Robinson, Steyn-Ross, and others.⁸⁻¹³ It has been used recently by Kramer *et al.*¹⁴ to study generalized seizure states in relation to epilepsy. We were at some pains to use realistic, physiologically derived values for the parameters of the model, as described in our previous articles. However, the question of accurate parametrization is still an open one because the measurements are typically derived from reported studies of single neurons, which are then assumed to be representative of average of the neural population. In brief, the model is formulated as a set of coupled differential equations in time and space that describe the time evolution of the mean soma potential of cortical “macrocolumns” of approximately 10^5 inhibitory and excitatory cortical neurons. The scalp electroencephalogram is an image of the time evolution of the summed mean soma potential of a large number of macrocolumns. In this way, the output from the theoretical model is a “pseudoelectroencephalogram” that can be directly compared with experimentally derived data that have been previously reported in the scientific literature. The differential equations also explicitly model action potential rates from cortical neuronal input. The distant input is modeled with a wave equation, and local input is modeled as an

instantaneous feedback (no reverberating cortex-thalamus loops are included). The shapes and time durations of the excitatory postsynaptic potentials (EPSPs), and IPSPs, are modeled with a second-order differential equation in time. Reversal potentials are used to modulate the resulting input to the cell membrane, thus constraining the mean membrane potentials to lie within certain bounds. A sigmoidal function is used to relate mean action potential rate to mean membrane potential in both excitatory and inhibitory neuronal populations. Subcortical neuronal input is included through a random noise term. Specifically, we used these equations to model the cortex in two spatial dimensions as a 50×50 -cm two-dimensional slab using periodic boundary conditions (approximately the area of unspecialized association cortex in humans). The quantitative effects of isoflurane and enflurane on IPSPs were incorporated using the data derived from Banks and Pearce⁴ in a manner similar to that of Bojak and Liley.¹⁵

Model Predictions

Enflurane versus Isoflurane

Examples of the pseudoelectroencephalogram generated by the model in response to changes in enflurane concentration are shown in figure 1. In simple terms, the behavior of the model cortex shows three main patterns: (1) an active higher-firing state that is similar to that observed in the alert cortex (fig. 2, area A), (2) a quiescent low-firing state that is similar to that described in cortical neurons that are under the influence of common γ -aminobutyric acid-mediated anesthetic drugs (fig. 2, area B), and (3) a state in which the cortex is unstable and oscillates rapidly between silence and supramaximal firing. We identify this state with seizures (fig. 2, area C).

We can now vary the amplitude and time duration of the IPSP to mimic the effects of increasing concentrations of enflurane and isoflurane on our model cortex, and then see what changes in the state of the cortical firing occur. As shown in figure 2, the effects of the anesthetic drugs are visualized using a plot of the decay time constant of the IPSP (y-axis) *versus* the time-integrated IPSP magnitude (x-axis). In essence, both enflurane and isoflurane cause an increase in total synaptic charge transfer (the area under each IPSP) of between 100 and 200%. This results in the cortex making a transition from an active state (fig. 2, area A)—which is identified as being the awake state—to a quiescent (anesthetized) state (fig. 2, area B).¹⁰ Figure 2b shows this transition more clearly by explicitly plotting the third dimension (the excitatory mean neuronal soma potential) along the z-axis. The trajectories followed by the model cortex in response to increasing concentrations of each anesthetic agent (enflurane = dashed line, isoflurane = solid line) are shown in figure 2. The start of each trajectory (bottom left) is zero anesthetic concentration,

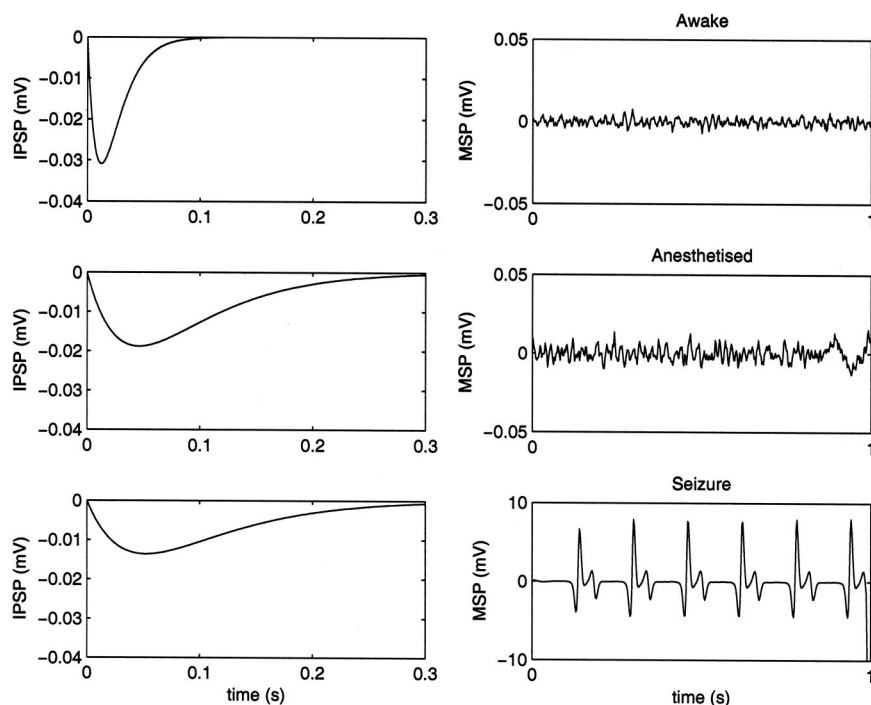


Fig. 1. Examples of fluctuations in mean soma potential (MSP) model output (“pseudoelectroencephalograms”), in response to changes in inhibitory postsynaptic potential (IPSP) input caused by enflurane. Anesthetized = 1 minimum alveolar concentration (MAC)₅₀ of enflurane; awake = zero enflurane; seizure = 2 MAC₅₀ of enflurane.

and the end of each trajectory (top right) is approximately 2 minimum alveolar concentration (MAC)₅₀. The point at which the anesthetic drug concentration equals 1 MAC₅₀ is shown by Xs near the apex of each trajectory. It can be seen that both isoflurane and enflurane cause the cortex to move from the awake state (area A) to the anesthetized state (area B). However, there is a region (area C) where the cortex undergoes a sudden change in

behavior to the unstable seizure state. Mathematically, the technical term for this is a subcritical Hopf bifurcation, to enter a limit-cycle oscillation. The figure shows that the enflurane trajectory has a greater probability of crossing, or entering, this unstable region, because enflurane reduces the IPSP magnitude more than isoflurane for a given IPSP time constant (*i.e.*, for an equal IPSP area, the shape of the enflurane-affected IPSP is “flatter” than that for isoflurane). When in this state (area C), the cortex alternates (approximately 5/s) abruptly between zero firing and supramaximal firing states, similar to that observed during seizures.^{16,17} The changes in stability of the cortical model were initially derived from analysis of the eigenvalues of the equations and then checked by the computer simulations. In addition to states similar to spike-wave seizures, spiral waves were also sometimes observed in the model when the trajectory crossed an unstable region. The shape of the IPSP is critical. Therefore, for a relative IPSP charge-transfer of two, the cortex could be either in a state of coma, if the IPSP was short and of high amplitude (fig. 2, position shown by diamond and subgraph ii), or in a seizure state, if the IPSP was long and of low amplitude (fig. 2, position shown by square and subgraph i). The model also predicts the propensity of enflurane to induce seizures in almost all cases at higher concentrations of above approximately 2%—where the trajectory turns back into the middle of the unstable region—as the total IPSP charge decreases in the presence of a slow IPSP decay time. This is because the effect of enflurane to decrease the peak amplitude of the IPSP is greater than its effect in prolonging the decay time. These results are in agreement with

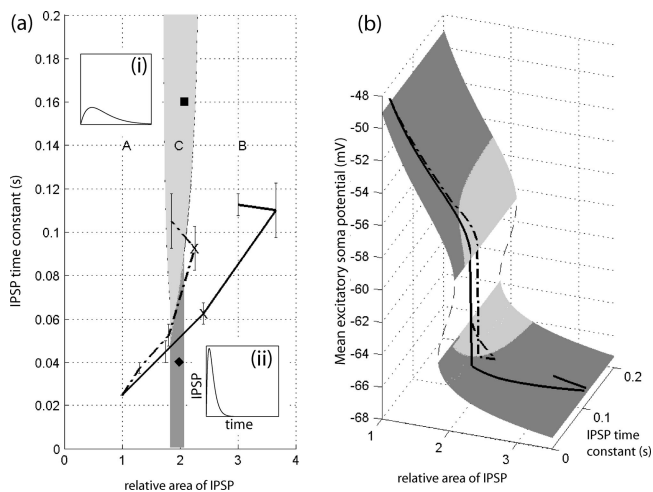


Fig. 2. A diagram of the stability of the modeled cortex as increasing concentrations of enflurane and isoflurane are applied. *b* shows a three-dimensional plot of the steady state excitatory neuronal soma potential. The dark shading and light shading denote stable (awake or anesthetized) and unstable (seizure) states, respectively. *a* shows a two-dimensional plan view of *b*. The trajectory of increasing concentrations (X = 1 minimum alveolar concentration₅₀) of enflurane is shown by the dashed line, and the trajectory of isoflurane is shown by the solid line. The insets show the (inverted) shape of the inhibitory postsynaptic potential (IPSP) at the points denoted by the square and diamond.

experimental observation¹⁸ and the theoretical work of Liley and Bojak.¹⁹

Although we have chosen our model parameters of the figure to make the difference in stability of the two trajectories obvious, the parameters are all physiologically plausible, and the implication that enflurane has the greater propensity to cause seizures is clear. Also note the magnitude of the uncertainties in the Banks and Pearce data. To check how robust the model is to changes of parameters, we performed 1,000 runs with different, but plausible, parameter sets. We find that, for isoflurane, the mean percentage of points on the trajectories lying in an unstable region is 2.8–3.0%, with a total of 50–52% of trajectories crossing the unstable area at some point on their path. (The range gives an indication of the standard uncertainty in the result.) For enflurane, the same values are 11.5–12.7% and 57–60%. Moreover, 4.9–6.3% of trajectories for enflurane were unstable over at least half of their length, whereas no occasions of such a large instability were recorded for isoflurane.

Interactions with Thiopentone

Counterintuitively, the addition of thiopentone—usually an efficacious antiepileptic drug—to low concentrations of enflurane has been shown to increase seizure activity.²⁰ Thiopentone prolongs the IPSP decay time but has no effect on the peak amplitude of the IPSP²¹ and therefore would generate a trajectory that travels up and rightward. From inspection of figure 2, it can be seen that the effect of adding thiopentone to a low concentration of enflurane could shift the enflurane trajectory up and to the right, thus causing it to be more likely to enter the oscillatory seizure state (the lower part of area C). Conversely, at higher concentrations of enflurane (> 2%), thiopentone has an anticonvulsant effect because it would shift the trajectory to the right, away from reentering area C.

Other Proconvulsant and Anticonvulsant Drug Interactions

The main interest of the model lies in its explanation of the proconvulsant effects of seemingly neurodepressant drugs. However, decreased excitation (modeled as shortening of the EPSP decay time constant and consequently a reduction in integrated magnitude) results in the area of instability (fig. 3A, area C) becoming narrower and moving upward and to the left. This explains the experimental observation that *N*-methyl-D-aspartate antagonist drugs effectively prevent or abort enflurane-induced convulsions.²² Simulations of *N*-methyl-D-aspartate blockade with an EPSP reduced in both area and time by 25% give just 19–21% of 1,000 simulated enflurane paths as crossing the unstable region, compared with 57–60% of enflurane paths without the *N*-methyl-D-aspartate blockade.

Equivalently, the increased inhibition of neuronal firing caused by opening of extrasynaptic γ -aminobutyric

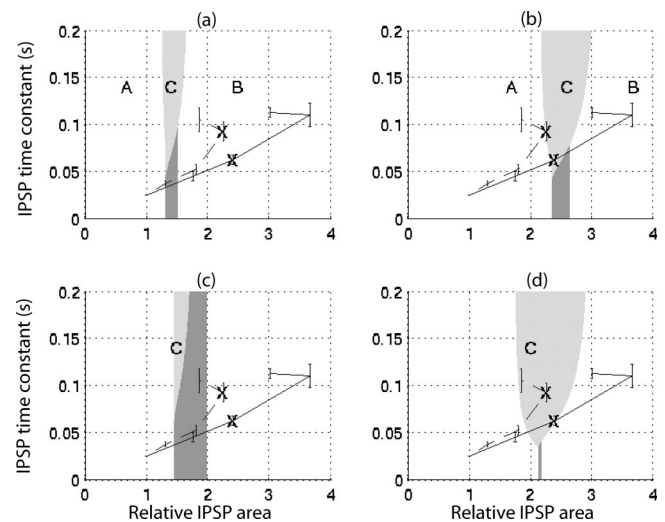


Fig. 3. Plots showing the effect of different adjunctive drugs on the unstable area (area C) of the relative inhibitory postsynaptic potential area versus inhibitory postsynaptic potential (IPSP) decay-time diagram. *a* shows the decrease in unstable area caused by *N*-methyl-D-aspartate blockade. *b* shows the increase in unstable area caused by augmented excitatory postsynaptic potential amplitude, such as might be induced by 5-(2-cyclohexylethyl)-5-ethyl barbituric acid. *c* shows the decrease in unstable area caused by augmentation of tonic hyperpolarizing (potassium or chloride) currents, amounting to a -2.0 -mV shift in resting potential. *d* shows the increase in unstable area caused by inhibition of tonic currents, amounting to a $+2.0$ -mV shift in resting potential. The trajectories are for increasing concentrations of isoflurane (solid line) and enflurane (dashed line), as in figure 2.

acid/Cl channels or potassium channels may be modeled as hyperpolarization of the resting membrane potential. This also causes the size of area C of figure 3 to decrease and shift to the left (fig. 3c). As an aside, it may be noted that both diminution of EPSP and resting membrane potential hyperpolarization also move the junction between the awake (area A) and anesthetized (area B) states to the left. This explains the fact that the anesthetic potency of volatile agents is increased by interactions with ketamine (an *N*-methyl-D-aspartate blocker) and with benzodiazepines (potent antiepileptic drugs that are known to increase tonic chloride currents).²³

Conversely, increased excitation induced by proconvulsant volatile “anesthetic” agents such as 5-(2-cyclohexylethyl)-5-ethyl barbituric acid²⁴ (modeled as a 25% increase in the area of the EPSP) cause a great increase in the area of the unstable region (fig. 3b, area C), such that it dominates the phase plane. Likewise, decreased tonic inhibition—such as may be induced by physostigmine or 4-amino-pyridine²⁵—may be modeled as depolarization of the resting membrane potential of the cortical neurons. This effect will greatly increase the propensity for the development of seizures (note large area C in fig. 3d).

Discussion

It is easy to imagine that seizures could occur when the balance between inhibition and excitation in the

cerebral cortex is unbalanced toward excessive excitation. It is less clear how seizures could occur when the cortex is in a predominantly inhibitory mode. Even this relatively simple model can quantitatively describe how it is possible for seizures to occur in an anesthetized cerebral cortex. It also shows that modest changes in the pattern of synaptic response can result in gross changes in the behavior of populations of neurons. The seizure state emerges as a natural consequence of the model dynamics. We contend that it is not possible to explain the phenomenon of seizures occurring in a quiescent cortex, without some attempt to model the interneuronal dynamical interactions. The critical factors are that (1) the system is in an inhibitory state and (2) there exists a disproportionate prolongation of the IPSP, which introduces a lag in the system, thus predisposing the cortex to oscillate. The impact of synaptic excitatory inputs on the generation of action potentials at the soma is controlled by complex active and passive, spatial and temporal filters in the dendritic tree.^{26,27} It may be surmised that other drugs and pathologic processes that slow or broaden the dendritic summation will have similar pro-seizure effects.

The parameters that control our model (*e.g.*, the various voltages; the size, number, and time courses of the synaptic events; see appendix) are derived as far as possible from data that have been experimentally verified in the peer-reviewed literature. However, there exists some uncertainty as to the exact values. We justify our choice of parameter values from three arguments: (1) The experimental measurements of neuron-by-neuron parameters that are reported in the literature seem to vary widely with time and context. Therefore, narrow limits in the variability of individual parameters are probably less physiologically critical than relations between groups of parameters. (2) The fact that the cortex can continue to function, to some degree, in the face of significant neurobiologic disturbances (*e.g.*, histamine or muscarinic blockade by drugs) argues that multiple parallel redundant pathways exist. (3) The cortex exhibits some degree of adaptive self-organization, which would hugely constrain the effective size of the parameter space.

In our model, we do not specifically include subcortical interactions, except as a source of nonspecific activating input and *via* the indirect effect of changes in neuromodulatory systems on the parameter values of the cortical neurons. There is strong experimental evidence that thalamocortical circuits are not essential for the development of seizures.¹⁷ We also assume that the only effect of the anesthetic drugs is on the IPSP, and we model the cortex as a simple two-dimensional sheet, without taking into consideration three-dimensional layering or variations between different regions within the cortex. These and other issues related to seizure onset and termination (such as second-order changes in chloride and potassium balance across the neuronal cellular

membrane) may be investigated in more detail in future models. For example, the exaggerated frontal electroencephalographic effects of common γ -aminobutyric acid-mediated anesthetic drugs would clearly indicate heterogeneity in parameters between frontal and occipital lobes. Similarly, most of the corticocortical axons interact with inhibitory interneurons and apical pyramidal cell dendrites in the superficial layers of the cortex (cortical layers 1 and 2), whereas axonal input from the thalamus occurs predominantly near the pyramidal cell bodies (cortical layers 3–5). However, even our simple model seems to have adequate explanatory power to describe most of the observed phenomena, because these phenomena (anesthesia and seizures) are global features of cortical function.

We conclude that the technique of mean-field modeling of the cerebral cortex is able to explain parsimoniously and elegantly a constellation of counterintuitive neuropharmacologic experimental data.

Appendix: Formulation of the Mean-field Model of Cortical Interactions

The model quantitatively describes the interactions between populations of excitatory pyramidal neurons (subscript *e*) and inhibitory interneurons (subscript *i*). We have used the convention of *a*→*b*, as meaning the direction of transmission in the synaptic connections is from the presynaptic nerve *a* to postsynaptic nerve *b*. The subscript *sc* indicates random subcortical input that is independent of the cortical membrane potential. The variables V_a and Φ_{ab} vary in time and space. The time evolutions of the mean neuronal soma membrane potential (V_a) in each population (excitatory [*e*] and inhibitory [*i*]) of neurons in response to synaptic input ($\rho_a \psi_{ab} \Phi_{ab}$) are given by the following set of equations:

$$\tau_e \frac{\partial V_e}{\partial t} = V_e^{rest} - V_e + \Delta V_e^{rest} + \lambda_{ACb} \rho_e \psi_{ee} \Phi_{ee} + \rho_i \psi_{ie} \Phi_{ie} \quad (\text{A1})$$

$$\tau_i \frac{\partial V_i}{\partial t} = V_i^{rest} - V_i + \lambda_{ACb} \rho_e \psi_{ei} \Phi_{ei} + \rho_i \psi_{ii} \Phi_{ii}, \quad (\text{A2})$$

where τ_a are the time constants of the neurons, ρ_a are the strength of the postsynaptic potentials (proportional to the total charge transferred), ψ_{ab} are the weighting functions that allow for the effects of reversal potentials and are described by the equation

$$\psi_{ab} = \frac{V_a^{rev} - V_b}{V_a^{rev} - V_a^{sc}}, \quad (\text{A3})$$

and Φ_{ab} are the synaptic input spike-rate densities (flux) that are described by the following equations:

$$\left(\frac{\partial^2}{\partial t^2} + 2\gamma_{ee} \frac{\partial}{\partial t} + \gamma_{ee}^2 \right) \Phi_{ee} = \gamma_{ee}^2 (N_{ee}^{\alpha} \Phi_{ee} + N_{ee}^{\beta} Q_e + \Phi_{ee}^{sc}) \quad (\text{A4})$$

$$\left(\frac{\partial^2}{\partial t^2} + 2\gamma_{ei} \frac{\partial}{\partial t} + \gamma_{ei}^2 \right) \Phi_{ei} = \gamma_{ei}^2 (N_{ei}^{\alpha} \Phi_{ei} + N_{ei}^{\beta} Q_e + \Phi_{ei}^{sc}) \quad (\text{A5})$$

$$\left(\frac{\partial^2}{\partial t^2} + 2\gamma_{ie} \frac{\partial}{\partial t} + \gamma_{ie}^2 \right) \Phi_{ie} = \gamma_{ie}^2 (N_{ie}^{\beta} Q_i + \Phi_{ie}^{sc}) \quad (\text{A6})$$

$$\left(\frac{\partial^2}{\partial t^2} + 2\gamma_{ii} \frac{\partial}{\partial t} + \gamma_{ii}^2 \right) \Phi_{ii} = \gamma_{ii}^2 (N_{ii}^{\beta} Q_i + \Phi_{ii}^{sc}) \quad (\text{A7})$$

Table 1. Parameter Values of the Model

Parameter	Description	Standard Values (<i>e, i</i>)
$\tau_{e,i}$	Membrane time constant	0.04, 0.04 s ⁻¹
$Q_{e,i}$	Maximum firing rates	30, 60 s ⁻¹
$\theta_{e,i}$	Sigmoid thresholds	-58.5, -58.5 mV
$\sigma_{e,i}$	SD for threshold	4.0, 6.0 mV
ρ_e	Gain per <i>e</i> synapse at resting voltage	0.001 mV · s
V_{rev}	Cell reversal (Nernst) potential	0, -70 mV
$V_{rest}^{e,i}$	Cell resting potential	-64, -64 mV
$N_{e,a}^{\alpha}$	Long-range <i>e</i> to <i>e</i> or <i>i</i> connectivity	3,710
$N_{e,i}^{\beta}$	Short-range <i>e</i> to <i>e</i> or <i>i</i> connectivity	410
$N_{i,a}^{\beta}$	Short-range <i>i</i> to <i>e</i> or <i>i</i> connectivity	800
$\langle \varphi_{ea}^{sc} \rangle$	Mean <i>e</i> to <i>e</i> or <i>i</i> subcortical flux	750 s ⁻¹
$\langle \varphi_{ia}^{sc} \rangle$	Mean <i>i</i> to <i>e</i> or <i>i</i> subcortical flux	1,500 s ⁻¹
$\gamma_{e,a}$	Excitatory synaptic rate constant	300 s ⁻¹
$L_{x,y}$	Spatial length of cortex in model	500 mm
$\alpha_{m,c}$	Area of macrocolumn	1 mm ²
$\Lambda_{e,a}$	Characteristic inverse length connection scale	0.2 mm ⁻¹
ν	Mean axonal conduction speed	1,400 mm/s
Altered parameter value ranges		
$\gamma_{i,a}$	Inhibitory rate constant in absence of anesthetic agent	60 to 100 s ⁻¹
ρ_i	Gain per <i>i</i> synapse at resting voltage	-0.0008 to -0.0013 mV · s
ν	Effect of axonal function impairment	1,000 to 5,000 mm/s
ΔV_{rest}	Effect of altering extrasynaptic ion channels	-2.0 to +2.0 mV
λ_{Ach}	Effect of muscarinic neuromodulation	1.0 to 1.5

The effect of the anesthetic is to scale $\gamma_{i,a}$ and ρ_i using the values obtained from the Banks and Pearce⁴ data.

where γ_{ab} are the synaptic rate constants, N^{α} is the number of long-range connections, and N^{β} is the number of local, intramacrocolumn connections. The mean axonal velocity is given by ν , and the characteristic length (the length at which the connectivity decays to $1/e$) is $1/\Lambda_{e,a}$. The spatial interactions among and within the macrocolumns are described by the two equations

$$\left(\frac{\partial^2}{\partial t^2} + 2\nu\Lambda_{ee}\frac{\partial}{\partial t} + \nu^2\Lambda_{ee}^2 - \nu^2\nabla^2 \right) \varphi_{ee} = \nu^2\Lambda_{ee}^2 Q_e \quad (A8)$$

$$\left(\frac{\partial^2}{\partial t^2} + 2\nu\Lambda_{ei}\frac{\partial}{\partial t} + \nu^2\Lambda_{ei}^2 - \nu^2\nabla^2 \right) \varphi_{ei} = \nu^2\Lambda_{ei}^2 Q_e \quad (A9)$$

The population firing rate of the neurons is related to their mean soma potential by sigmoidal functions

$$Q_e(V_e) = \frac{Q_e^{\max}}{1 + \exp[-\pi(V_e - \theta_e)/\sqrt{3}\sigma_e]} \quad (A10)$$

$$Q_i(V_i) = \frac{Q_i^{\max}}{1 + \exp[-\pi(V_i - \theta_i)/\sqrt{3}\sigma_i]} \quad (A11)$$

where θ_a describes the inflection point voltage, and σ_a describes the SD of the threshold potential. The parameters and ranges used in our simulations are shown in table 1 (*e* and *i* refer to values assigned to excitatory and inhibitory cell populations).

References

1. Modica PA, Tempelhoff R, White PF: Pro- and anticonvulsant effects of anesthetics: I. *Anesth Analg* 1990; 70:303-15
2. Modica PA, Tempelhoff R, White PF: Pro- and anticonvulsant effects of anesthetics: II. *Anesth Analg* 1990; 70:433-44
3. Oshima E, Urabe N, Shingu K, Mori K: Anticonvulsant actions of enflurane on epilepsy models in cats. *ANESTHESIOLOGY* 1985; 63:29-40
4. Banks MI, Pearce RA: Dual actions of volatile anesthetics on GABA_A IPSCs: Dissociation of blocking and prolonging effects. *ANESTHESIOLOGY* 1999; 90:120-34
5. Tas PW, Roewer N: The volatile anesthetic enflurane activates capacitative Ca²⁺ channels in rat glioma C6 cells. *Toxicol Lett* 1998; 100-101:265-9
6. McCormick DA, Contreras D: On the cellular and network bases of epileptic seizures. *Annu Rev Physiol* 2001; 63:815-46
7. Wilson MT, Steyn-Ross ML, Steyn-Ross DA, Sleight JW: Predictions and

- simulations of cortical dynamics during natural sleep using a continuum approach. *Phys Rev E (Stat Nonlin Soft Matter Phys)* 2005; 72:051910
8. Steyn-Ross ML, Steyn-Ross DA, Sleight JW: Modelling general anaesthesia as a first-order phase transition in the cortex. *Prog Biophys Mol Biol* 2004; 85:369-85
9. Liley DT, Cadusch PJ, Gray M, Nathan PJ: Drug-induced modification of the system properties associated with spontaneous human electroencephalographic activity. *Phys Rev E (Stat Nonlin Soft Matter Phys)* 2003; 68:051906
10. Steyn-Ross ML, Steyn-Ross DA, Sleight JW, Liley DT: Theoretical electroencephalogram stationary spectrum for a white-noise-driven cortex: Evidence for a general anesthetic-induced phase transition. *Phys Rev E (Stat Phys Plasmas Fluids Relat Interdiscip Topics)* 1999; 60:7299-311
11. Liley DT, Cadusch PJ, Dafilis MP: A spatially continuous mean field theory of electrocortical activity. *Network* 2002; 13:67-113
12. Wright JJ, Rennie CJ, Lees GJ, Robinson PA, Bourke PD, Chapman CL, Gordon E, Rowe DL: Simulated electrocortical activity at microscopic, mesoscopic, and global scales. *Neuropsychopharmacology* 2003;28 (suppl 1):S80-93
13. Robinson PA, Rennie CJ, Rowe DL: Dynamics of large-scale brain activity in normal arousal states and epileptic seizures. *Phys Rev E (Stat Nonlin Soft Matter Phys)* 2002; 65:041924
14. Kramer MA, Kirsch HE, Szeri AJ: Pathological pattern formation and epileptic seizures. *J R Soc Lond* 2005; 2:113-27
15. Bojak I, Liley DTJ: Modeling the effects of anesthesia on the electroencephalogram. *Phys Rev E (Stat Nonlin Soft Matter Phys)* 2005; 71:041902
16. Steriade M, Amzica F: Intracellular study of excitability in the seizure-prone neocortex *in vivo*. *J Neurophysiol* 1999; 82:3108-22
17. Timofeev I, Steriade M: Neocortical seizures: Initiation, development and cessation. *Neuroscience* 2004; 123:299-336
18. Stevens JE, Fujinaga M, Oshima E, Mori K: The biphasic pattern of the convulsive property of enflurane in cats. *Br J Anaesth* 1984; 56:395-403
19. Liley DT, Bojak I: Understanding the transition to seizure by modeling the epileptiform activity of general anaesthetic agents. *J Clin Neurophysiol* 2005; 22:300-13
20. Furgang FA, Sohn JJ: The effect of thiopentone on enflurane-induced cortical seizures. *Br J Anaesth* 1977; 49:127-32
21. Lukatch HS, MacIver MB: Synaptic mechanisms of thiopental-induced alterations in synchronized cortical activity. *ANESTHESIOLOGY* 1996; 84:1425-34
22. MacIver MB, Kendig JJ: Enflurane-induced burst discharge of hippocampal CA1 neurones is blocked by the NMDA receptor antagonist APV. *Br J Anaesth* 1989; 63:296-305
23. Yeung JY, Canning KJ, Zhu G, Pennefather P, MacDonald JF, Orser BA: Tonically activated GABAA receptors in hippocampal neurones are high-affinity, low-conductance sensors for extracellular GABA. *Mol Pharmacol* 2003; 63:2-8
24. Wei L, Schlame M, Downes H, Hemmings HC: CHEB, a convulsant barbiturate, evokes calcium-dependent spontaneous glutamate release from rat cerebrocortical synaptosomes. *Neuropharmacology* 1996; 35:695-701
25. Netoff TI, Schiff SJ: Decreased neuronal synchronization during experimental seizures. *J Neurosci* 2002; 15:7297-307
26. Stuart G, Schiller J, Sakmann B: Action potential initiation and propagation in rat neocortical pyramidal neurons. *J Physiol* 1997; 15:617-32
27. Williams SR, Stuart GJ: Role of dendritic synapse location in the control of action potential output. *Trends Neurosci* 2003; 26:147-54